



# Using a novel optimization algorithm for parameter extraction of photovoltaic cells and modules

Nafiseh Pourmousa<sup>1,a</sup>, S. Mohammadreza Ebrahimi<sup>2</sup>, Milad Malekzadeh<sup>3</sup>, Francisco Gordillo<sup>4</sup>

<sup>1</sup> Department of Electrical Engineering, Iran University of Science and Technology, Tehran, Iran

<sup>2</sup> Department of Electrical Engineering, Babol Noshirvani University of Technology, Babol, Iran

<sup>3</sup> Dynamic Systems and Simulation Laboratory, Technical University of Crete, Chania, Greece

<sup>4</sup> Department of Systems Engineering and Automatic Control, Universidad de Sevilla, Sevilla, Spain

Received: 4 April 2021 / Accepted: 19 April 2021

© The Author(s), under exclusive licence to Società Italiana di Fisica and Springer-Verlag GmbH Germany, part of Springer Nature 2021

**Abstract** The critical worldwide revolution towards clean energy has prompted the improvement of studies on the fabrication of high-performance solar cells. In this regard, rendering an accurate model of the solar cell for performance evaluation in the simulation could be essential. So far, several models have been proposed for the solar cell, including single-diode model (SDM), double-diode model (DDM), and three-diode model (TDM). By increasing the number of diodes considered in the equivalent circuit in order to deliver a more accurate model, the number of unknown parameters which must be identified will be increased as well. Therefore, presenting an efficient algorithm to estimate these parameters becomes an interesting issue in recent years. In this study, an improved optimization algorithm, called springy whale optimization algorithm (SWOA), is proposed to estimate the model parameters of solar cells. SWOA is a generalization of the WOA and has the advantages of high convergence speed, global search capability, and high robustness over it. In order to inquire the efficiency of SWOA, this algorithm is posed to estimate the parameters of models of solar cells and photovoltaic (PV) modules as well; the simulation results authenticate the supremacy of the proposed algorithm. Furthermore, the effectiveness of SWOA algorithm in the practical application has been evaluated using commercial modules, including polycrystalline (SW255), multi-crystalline (KC200GT), and monocrystalline (SM55). This assessment is carried out for various operating conditions under different irradiance and temperature conditions, which yield variations in the parameters of the PV model. The results obtained from various experimental setups confirm the high performance and robustness of the proposed algorithm.

## 1 Introduction

Nowadays, it can be heard that renewable energy such as solar and wind must be taken into account instead of conventional fossil and nuclear energy in order to save the world from pollution and irrevocable damages. To use solar energy, we must be able to convert this

<sup>a</sup> e-mail: [n\\_pormousa@alumni.ac.ir](mailto:n_pormousa@alumni.ac.ir) (corresponding author)

energy into other forms that can be used in everyday life with the help of a suitable tool [1, 2]. Photovoltaic (PV) solar systems are a good tool to catch solar energy for electrical energy transformation. Solar cells can be produced with different technologies and some of these technologies, such as silicon cells, have matured and are widely used [3, 4]. Increasing the efficiency and reliability of these technologies is one of the concerns of scientists. Understanding the processes related to power absorption and conversion in these cells and accurate modeling can play an effective role in their proper prediction and design. Building a reliable model of a solar module is one of the most important issues that researchers in photovoltaic systems are looking for [5–7]. This model will be especially important when studying the characteristics of the photovoltaic system.

Predicting the output power of the system and creating a system that can extract the maximum power, such as tracking the maximum power point, are features that photovoltaic system modeling can help a lot [8]. A key issue in modeling photovoltaic modules is the nonlinear relationship between current and output voltage, especially when solar arrays are affected by rapidly changing weather conditions and shading [9, 10]. The main problem in modeling is to identify the optimal values of the parameters by which the model best fits the experimental data [8]. Also, to better understand the characteristics, evaluating the optimization performance of a solar cell system, a precise mathematical model has a significant role for researchers. Different models have been used to show the behavior of the system in different operating conditions. These models range from simple hypotheses to models with complex physical variables [11, 12]. The precision of these models is intent by the model parameters, because some of the necessary information for optimization is not announced in the data sheet provided by the factory. For this reason, it is necessary to obtain these parameters, which may be turned into an optimization problem with a specific objective function [13].

In recent decades, several methods have been used to determine the optimal values in solar cell models, which can be divided into conventional and heuristic algorithms [14, 15]. Conventional methods require coherence and derivability to be practical, involve heavy computations, and converge to local and local solutions instead of global solutions [16]. The nonlinearity of the curve (I–V) makes conventional optimization techniques incapable of effectively solving parameter recognition problems [17]. To address this issue, heuristic optimization algorithms such as genetic algorithm, PSO algorithm, etc., have been used to identify the parameters [18, 19]. Although these algorithms have better results than traditional algorithms, they have some limitations, the most important of which are their entrapment in local optimal points and early convergence to these points.

So far, several models have been introduced for solar cells, the most important of which are single-diode model (SDM), double-diode model (DDM), and three-diode model (TDM) [20, 22]. Various algorithms have been posed to estimate the parameters of these models, and many articles in this field have been published with appropriate results, but improving the performance of algorithms and providing an algorithm with better convergence is still a topic of interest for researchers in this field. In this regard, different kinds of optimization algorithms can be found in literature such as genetic algorithms [18], sunflower optimization algorithm [23], flexible particle swarm optimization algorithm [24], coyote optimization algorithm [25], PG JAYA algorithm [26], lozi map [13], flower pollination algorithm [27], artificial bee swarm optimization (ABSO) [28], generalized oppositional teaching–learning based optimization (GOTLBO) [29], whale optimization algorithm [30], chaotic whale optimization [31], and so on [32–34].

One of the newest methods introduced is the whale optimization algorithm (WOA) presented by [30]. WOA imitates the behavior of humpback whales. These whales detect the position of the prey and then surround them. The WOA algorithm first finds the best search

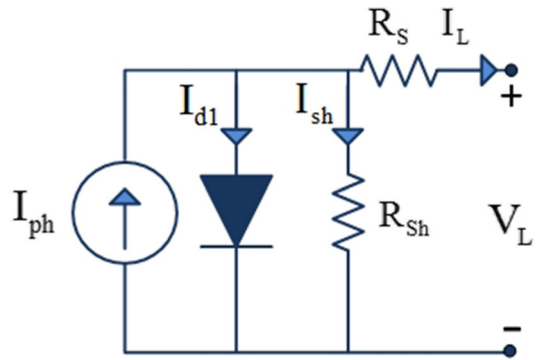
agent by producing whales and randomly distributing them in the search space. After that, other search agents try to update their positions according to the best achievement. This algorithm has been given a lot of attention in optimization issues, including solar cells and fuel cells parameters extraction and parameters estimation of DC motors [35], designing photonic crystal filter [36], neural networks, and computing [37, 38], maximum power point tracking [39–41], terminal voltage control [42], economic prediction [43, 44], and other world problems [45–47]. Although WOA has performed better than previous algorithms in solving complex nonlinear problems and multi-model objective function value, it still has difficulty finding optimal solutions. In the algorithm presented in [31], the main idea is the use of irregular maps to calculate and automatically attune the internal parameters of the algorithm. This solution is very useful in complicated problems because; during the iteration process, this scheme enhances the ability of internal parameters to explore for the best solution, which increases the efficiency of the algorithm. Although the CWOA algorithm tries to unravel the problem of getting stuck in the local minimum, there is still the problem that points that are far from the optimal points are ignored from the optimization cycle, which can decline the search capability of the algorithm in complicated optimization problems. In this regard, a modified version of WOA called a springy whale optimization algorithm (SWOA) is presented as a modified optimization algorithm to extract the parameters of PV cell and module models in this study. To ameliorate the performance of the algorithm, some changes have been made in the movement of the whales. A removal phase has been added to apply changes to the whale algorithm. In the first step of each phase, a predetermined number of the worst whales are always removed and new whales are replaced in the new search space. Making these modification to the algorithm reduces the likelihood of being trapped in local minimums and elevates the rapidity of detecting optimal solutions. Furthermore, by removing points that are far from the optimal parameters, we can enhance the search capability of the proposed algorithm. To assess the sufficiency of the proposed algorithm, the performance of this algorithm is tested in different scenarios derived from laboratory information.

The continuation of this article as follows. Section 2 presents the mathematical relationships governing cell models and PV modules. Section 3 hands out the general concepts of the WOA algorithm. The principle idea about SWOA is given in detail in Sect. 4. Section 5 renders some simulation results regarding the experimental data set. Finally, Sect. 6 is devoted to the conclusion.

## 2 Photovoltaic modeling and problem formulation

Several models of solar cells have been proposed so far that take into account the physical losses of the solar cell, the most important of which are the SDM, DDM, and TDM. The SDM only takes into account losses caused by internal resistors, connections, and connecting lines between each solar cell and the module, so it does not have good accuracy. However, in the more complex models mentioned, in addition to internal losses and connections, losses such as leakage circuiting current and grain boundary are also considered. For this reason, the DDM and TDM are more accurate than SDM. In the following, we will examine the mathematical relationships governing the models and present the formulation of the problem.

**Fig. 1** Equivalent circuit of the single-diode model



2.1 Photovoltaic cell model

2.1.1 Single-diode model (SDM)

The SDM includes a current source, a diode that produces the distributed current component, and resistors  $R_s$  and  $R_{sh}$  which are responsible for losses caused by internal resistors, connections, and other connecting lines between each solar cell and the module, respectively [20]. The typical model of a single-diode solar cell is demonstrated in Fig. 1, where the output current ( $I_L$ ) from the solar cell is the current produced by the current generator ( $I_{ph}$ ) minus the currents flowing through the diode  $I_{d1}$  and the shunt resistor ( $I_{sh}$ ), respectively.

In many articles, this model is referred to as the five-parameter model, because in this model, five parameters exist and can be represented by the vector  $\theta$  as follows:

$$\theta = [ I_{ph} \ R_s \ R_{sh} \ I_{SD} \ n ] \tag{1}$$

The equations of the practical model of a single diode are as follows:

$$I_L = I_{ph} - I_D - I_{sh} \tag{2}$$

The diode current  $I_D$  is expressed by the Shockley equation as:

$$I_D = I_{SD} \left[ \exp\left(\frac{(V_L + I_L R_s)}{n V_T}\right) - 1 \right] \tag{3}$$

$$V_T = \frac{KT}{q}$$

Furthermore,  $I_{sh}$  is calculated from the following equation:

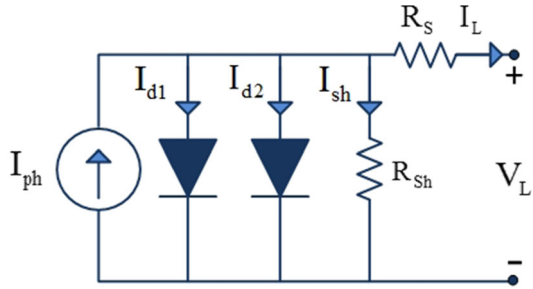
$$I_{sh} = \frac{V_L + I_L R_s}{R_{sh}} \tag{4}$$

By combining Eqs. (1)–(4), the output current of the diode is obtained as follows:

$$I_L = I_{ph} - I_{SD} \left[ \exp\left(\frac{q(V_L + I_L R_s)}{nKT}\right) - 1 \right] - \frac{V_L + I_L R_s}{R_{sh}} \tag{5}$$

where  $I_{SD}$  is the reverse saturation current of the diode,  $V_T$  is thermal voltage equivalent,  $K$  is the Boltzmann’s constant ( $q$  is the electronic charge,  $n$  is the diode ideality factor, and  $T$  is the absolute temperature of the p–n junction in Kelvin,  $R_{sh}$  is the shunt resistance, and  $R_s$  is the series resistance.

**Fig. 2** Equivalent circuit of the double-diode model



2.1.2 Double-diode model (DDM)

This model consists of a current source, series, and parallel resistors as well as two diodes. Figure 2 shows a DDM of a solar cell. In this model, another diode is added to the SDM, which is placed parallel to the SDM to transmit losses due to carrier recombination in the depletion layer and surface recombination which is defined by  $I_{d2}$  [21]. The current of the first diode ( $I_{d1}$ ) represents the current component, which is similar to the current  $I_{d1}$  in the single-diode model.

Because another diode is attached to the model, the number of parameters will also change, and in this model, seven parameters will be identified and optimized, which are given as vectors in Eq. (6). Hence, we will encounter more challenging optimization problems.

$$\theta = [ I_{ph} \ R_s \ R_{sh} \ I_{SD1} \ I_{SD2} \ n_1 \ n_2 ] \tag{6}$$

Using KCL law, the total output current for a solar cell will be calculated from Eq. (7):

$$I_L = I_{ph} - I_{D1} - I_{D2} - I_{sh} \tag{7}$$

Thus, the output current may be redefined as:

$$I_L = I_{ph} - I_{SD1} \left[ \exp \left( \frac{q(V_L + I_L R_s)}{n_1 kT} \right) - 1 \right] - I_{SD2} \left[ \exp \left( \frac{q(V_L + I_L R_s)}{n_2 kT} \right) - 1 \right] - \frac{V_L + I_L R_s}{R_{sh}} \tag{8}$$

2.1.3 Three-diode model (TDM)

Another model presented in [22] is the TDM, which takes into account more losses in comparison with two previous models of solar cells. According to Fig. 3, this model consists of a current source, three diodes, and two resistors. Like DDM, two diodes are included in the model due to losses of recombination and connections, and a third diode due to losses due to recombination defect regions and grain boundary.

This model contains nine parameters that have to be identified. They can be combined in the following vector:

$$\theta = [ I_{ph} \ R_s \ R_{sh} \ I_{SD1} \ I_{SD2} \ I_{SD3} \ n_1 \ n_2 \ n_3 ] \tag{9}$$

Using KCL law, the total output current for a solar cell will be calculated from Eq. (10):

$$I_L = I_{ph} - I_{D1} - I_{D2} - I_{D3} - I_{sh}. \tag{10}$$

**Fig. 3** Equivalent circuit of the three-diode model

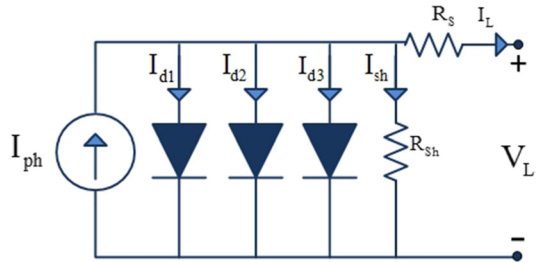
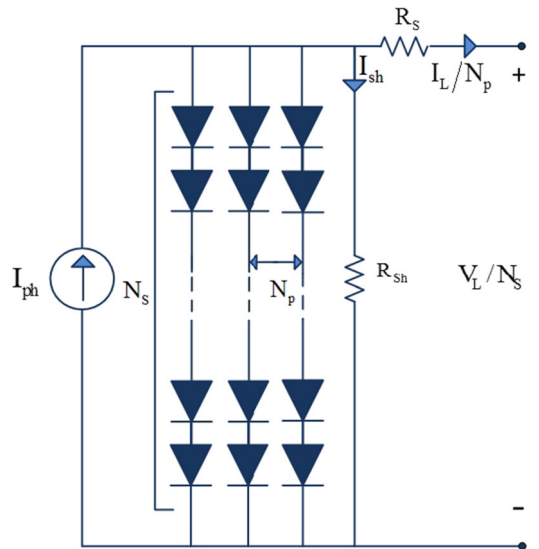


**Fig. 4** Equivalent circuit of solar PV module model



Thus, the output current may be redefined as:

$$\begin{aligned}
 I_L = & I_{ph} - I_{SD1} \left[ \exp\left(\frac{q(V_L + I_L R_s)}{n_1 kT}\right) - 1 \right] - I_{SD2} \left[ \exp\left(\frac{q(V_L + I_L R_s)}{n_2 kT}\right) - 1 \right] \\
 & - I_{SD3} \left[ \exp\left(\frac{q(V_L + I_L R_s)}{n_3 kT}\right) - 1 \right] - \frac{V_L + I_L R_s}{R_{sh}}
 \end{aligned} \tag{11}$$

It should also be noted that analytical modeling of the three-diode model is difficult due to a large number of parameters (nine parameters) and the small number of nonlinear equations.

### 2.2 Module model

In PV systems, the smallest unit includes several cells connected in series or in parallel to produce more power and output current. This set of cells is known as a module. Figure 4 shows a module.

As we know, the current of each cell is the same, and the output current of each of them is equal to  $I_L$ ; as a result, the output current ratio of the module can be written as Eq. (12).

$N_S$  is the number of solar cells in series, and  $N_P$  is the number of solar cells in parallel. It is obvious that five unknown parameters ( $I_{ph}$ ,  $I_{SD}$ ,  $R_s$ ,  $R_{sh}$ ,  $n$ ) need to be identified.

$$I_L = N_P \cdot I_{ph} - N_P \cdot I_{SD} \left[ \exp \left( \frac{q(V_L/N_S + I_L \cdot R_s/N_P)}{nKT} \right) - 1 \right] - \frac{N_P \cdot V_L/N_S + I_L \cdot R_s}{R_{sh}} \tag{12}$$

### 2.3 Objective function

The objective is to estimate the parameter values of the PV models in such a way that the values obtained from the model are as closest as possible to the measured data. For this, objective functions to be minimized for SDM, DDM and TDM are defined from (13) to (15), respectively:

$$\begin{cases} f_k(V_L, I_L, \theta) = I_{ph} - I_{SD} \left[ \exp \left( \frac{q(V_L + I_L R_s)}{nKT} \right) - 1 \right] - \frac{V_L + I_L R_s}{R_{sh}} - I_L \\ \theta = [I_{ph} \ R_s \ R_{sh} \ I_{SD} \ n] \end{cases} \tag{13}$$

$$\begin{cases} f_k(V_L, I_L, \theta) = I_L = I_{ph} - I_{SD1} \left[ \exp \left( \frac{q(V_L + I_L R_s)}{n_1 kT} \right) - 1 \right] \\ - I_{SD2} \left[ \exp \left( \frac{q(V_L + I_L R_s)}{n_2 kT} \right) - 1 \right] - \frac{V_L + I_L R_s}{R_{sh}} \\ \theta = [I_{ph} \ R_s \ R_{sh} \ I_{SD1} \ I_{SD2} \ n_1 \ n_2] \end{cases} \tag{14}$$

$$\begin{cases} f_k(V_L, I_L, \theta) = I_L = I_{ph} - I_{SD1} \left[ \exp \left( \frac{q(V_L + I_L R_s)}{n_1 kT} \right) - 1 \right] - I_{SD2} \left[ \exp \left( \frac{q(V_L + I_L R_s)}{n_2 kT} \right) - 1 \right] \\ - I_{SD3} \left[ \exp \left( \frac{q(V_L + I_L R_s)}{n_3 kT} \right) - 1 \right] - \frac{V_L + I_L R_s}{R_{sh}} \\ \theta = [I_{ph} \ R_s \ R_{sh} \ I_{SD1} \ I_{SD2} \ I_{SD3} \ n_1 \ n_2 \ n_3] \end{cases} \tag{15}$$

Then, as shown in Eq. (16) [11, 48], by minimizing, the calculated root mean square error (RMSE) is considered as the ultimate goal.

Consequently, parameter can be extracted by minimizing the objective function by seeking for the answer vector  $\theta$  within the limited area of practical parameters.

$$RSME(\theta) = \sqrt{\frac{1}{N} \sum_{i=1}^N f_k(V_L, I_L, \theta)^2} \tag{16}$$

where  $N$  shows the number of experimental data,  $\theta$  is the decision variable,  $V_L$ , and  $I_L$  are the measured voltage and current.

### 3 Data

Whales are extremely intelligent and emotional animals. The spindle-shaped cells that exist in certain areas of their brain have developed traits such as the ability to think, learn, judge, and social behaviors. Whales can hunt their prey individually and in groups. Some species

can live with their families all their lives. One of the largest toothless whales is called the humpback whale. The most fascinating factor about humpback whales is how they hunt [30].

The whale optimization algorithm simulates the behavior of humpback whales. These whales detect the position of the prey and then surround them. The WOA algorithm finds the best search agent after producing whales and randomly distributing them in the search space. After that, other search agents try to update their positions according to the best search agent. This behavior can be represented by the following equations [30]:

$$\vec{D} = \left| \vec{C} \cdot \vec{X}^*(t) - \vec{X}(t) \right| \quad (17)$$

$$\vec{X}(t+1) = \vec{X}^*(t) - \vec{A} \cdot \vec{D} \quad (18)$$

where  $t$  is the current iteration,  $\vec{A}$  and  $\vec{C}$  is the coefficient vectors,  $\vec{X}^*(t)$ , the location vector represents the best answer ever obtained,  $\vec{X}(t)$  is the vector of place,  $||$  is the absolute value, and  $\cdot$  represents the multiplication of element by element multiplication. It is important to note that if there is a better answer in each iteration,  $\vec{X}^*(t)$  then should be updated.

The vectors  $\vec{A}$  and  $\vec{C}$  are obtained using the following formulas:

$$\vec{A} = 2\vec{a} \cdot \vec{r} - \vec{a} \quad (19)$$

$$\vec{C} = 2 \cdot \vec{r} \quad (20)$$

where  $\vec{a}$  represents a linear decrease from 2 to zero during the iterations (both in the exploration and the exploitation phases) and  $\vec{r}$  represents a random vector in the interval  $[0,1]$ . By setting the random values of  $\vec{A}$  in the interval  $[-1, 1]$ , we can define the new location of the search agent anywhere between the initial position of the agent and the position of the best current agent.

Equation (18) will allow each search agent to update its position in the neighborhood of the current best answer and simulate looping around the prey.

Humpback whales, in addition to the looping strategy around the prey, can also have a spiral motion towards it. This motion can be simulated with the following formula [30]:

$$\begin{aligned} \vec{X}(t+1) &= \vec{D}^\circ \cdot e^{bl} \cdot \cos(2\pi l) + \vec{X}^*(t) \\ \vec{D}^\circ &= \left| \vec{X}^*(t) - \vec{X}(t) \right| \end{aligned} \quad (21)$$

where  $\vec{D}^\circ = \left| \vec{X}^*(t) - \vec{X}(t) \right|$  and indicates the distance of the  $i$ th wale to the prey (best solution obtained so far),  $b$  represents a constant that will denote the shape of a logarithmic helix, and  $l$  represents a random number in the interval  $[-1,1]$ .

Note that the humpback whales move around the prey simultaneously, both in the form of a contractile circle and along a spiral path. To model this simultaneous behavior, we assume that there is a 50% probability that the contractile loop mechanism or spiral model can be used to improve the position of the whales during optimization. The mathematical model is as follows:

$$\vec{X}(t+1) = \begin{cases} \vec{X}^*(t) - \vec{A} \cdot \vec{D} & \text{if } p \geq 0.5 \\ \vec{D}^\circ \cdot e^{bl} \cdot \cos(2\pi l) + \vec{X}^*(t) & \text{if } p < 0.5 \end{cases} \quad (22)$$

where  $p$  represents a random number in the interval  $[0,1]$ .

In addition to the bubble net method, humpback whales randomly search for prey. They search randomly, based on each other's position. In order to create a new paradigm in optimization policy, the random value is taken into account for  $\vec{A}$  (higher than 1 and lower than



–1) to follow a new position in the search area. This mechanism allows the WOA algorithm to perform a global search. The mathematical model of this work will be as follows [30]:

$$\vec{D} = \left| \vec{C} \cdot \vec{X}_{\text{rand}} - \vec{X}(t) \right|$$

$$\vec{X}(t+1) = \vec{X}_{\text{rand}} - \vec{A} \cdot \vec{D} \quad (23)$$

where  $\vec{X}_{\text{rand}}$  represents a random location vector (a random whale) selected from the current population.

#### 4 Springy whale algorithm (SWOA)

Although the whale algorithm has a high rate of convergence, it is stuck in local minima and thus in some cases does not converge to the global minimum. This problem manifests itself better when the amount of unknown parameters to identify is large. In the proposed scheme, changes have been made in the process of moving the whales towards the desired answer so as to improve the performance of the algorithm. A removal phase has been added to the classic whale algorithm to apply the changes. Toward the start of each stage, a certain number of the worst whales will be removed and substituted by new whales in the new search space. Making new early populations allows whales to acquire new ways to get the best response. Regarding this amendment, the probability of being trapped in local minima decreases, and the rapidity of detecting optimal solutions increases.

Preliminary, Elimination Period (*ep*) (this parameter is added to the classical algorithm and is defined based on the number of iterations) and elimination percent (*et*) (this parameter is added to the classical algorithm and is determined based on the initial population percentage) are set.

(*Th*) represents the percentage of the maximum or minimum of the search space. For instance, let us define  $Th = 95$  and the initial search space for the parameters is in the interval  $[-1, 1]$ . In each elimination phase, the value of each parameter in the particle is checked, and if it is greater than 95% of the absolute value of the search space, then one unit adds to the search space of that parameter.

The implementation steps of the improved whale algorithm are shown in Fig. 5. The changes applied to the classical algorithm by the blue blocks are shown in this figure.

A prospect of the usage of this method of identifying the unknown parameters of the solar cell system is given in Fig. 6. According to Fig. 6, after repeating the algorithm, each time, the error between the measured current and the extracted current is determined, and by placing this value in Eq. (16), the RMSE will be calculated. The purpose of modifying the classical whale algorithm and to introduce the SWOA algorithm was to minimize the RMSE value.

#### 5 Experimental results and discussions

In this section, to evaluate the performance of the proposed algorithm, we identify the parameters of the solar cell model and the PV module using the SDM, the DDM, the TDM, and the module model. Voltage–current experimental data from [24, 26] have been chosen as criterion used to test and contrast different methods. These data relate to a commercial silicon solar cell (French RTC Company) with a diameter of 57 mm, at a temperature of 33 °C and 1 sun (1000 w/m<sup>2</sup>) and a commercial solar module called Photowatt-PWP201 with 36 polycrystalline cell series at a temperature of 45 °C and 1 sun (1000 w/m<sup>2</sup>). Then, the

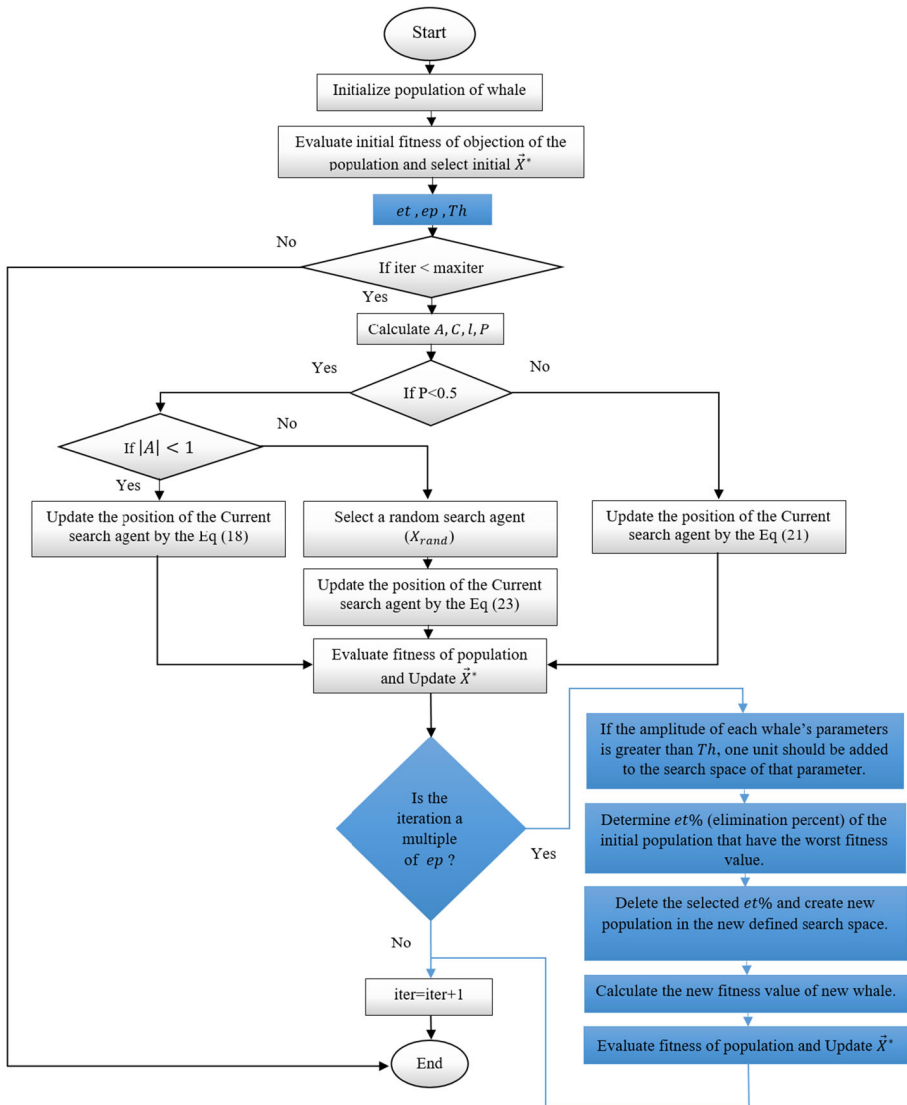
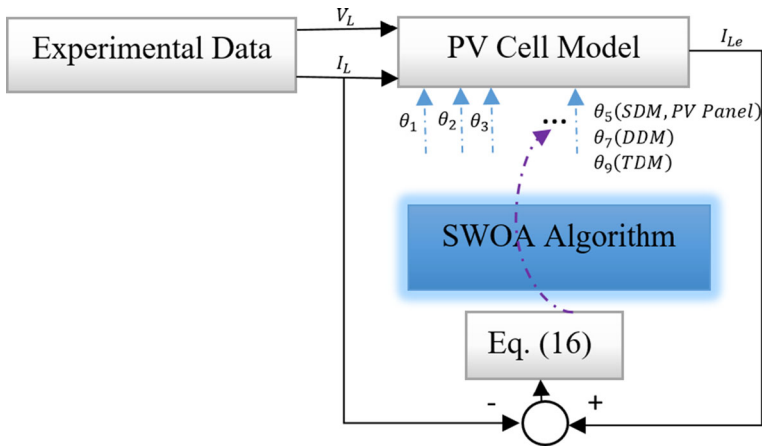


Fig. 5 Flowchart of the SWOA algorithm

parameters of three types of widely used modules called polycrystalline (SW255), multi-crystalline (KC200GT), and monocrystalline (SM55) have been identified under different radiation and temperature conditions. Then, to test the accuracy of the parameters identified in standard radiation and temperature ( $T_{STC} = 25^{\circ}C$ ,  $G_{STC} = 1000w/m^2$ ), the behavior of the relevant module was investigated in different radiation and temperature. As a result, it was observed that its behavior with the appropriate error is similar to the diagrams in the module datasheet [9, 49]. Also, the simulation results will be associated with comparing SWOA and some algorithms mentioned in the previous section. These tests were performed in MATLAB 2016b.



**Fig. 6** Overview for parameters estimation of PV Cell models using SWOA

**Table 1** Parameters ranges of RTC France PV cell and PV module [26]

Parameter	RTC France PV		PWP201		PV module	
	Lower value	Upper value	Lower value	Upper value	Lower value	Upper value
$I_{ph}(A)$	0	1	0	2	0	$2 I_{SC}$
$I_{sd1}, I_{sd2}, I_{sd3}(\mu A)$	0	1	0	50	0	100
$R_s(\Omega)$	0	0.5	0	2	0	2
$R_{sh}(\Omega)$	0	100	0	1000	0	5000
$n_1, n_2$	1	2	1	50	1	4
$n_3$	2	5	1	50	–	–

To ensure that the exploration space for each problem is identical, the domains correlated with each parameter are maintained as used in the previous literature. Table 1 demonstrates the limited areas for each parameter of the PV cell model and module [26].

In this paper, for a broader comparison, the algorithms used in each section are different. With the exception of the number of iterations and the number of populations, which are estimated at 5,000 and 30, respectively, the other parameters of the algorithm are set based on the main reference.

### 5.1 Parameters of RTC France solar cell

In Table 2, the results for estimating the 5 parameters for the SDM are given by SWOA and 10 other algorithms called whale optimization algorithm (WOA) [30], chaotic whale optimization algorithm (CWOA) [31], performance-guided JAYA(PGJAYA) [26], flexible particle swarm optimization (FPSO) [24], improved JAYA (IJAYA) [16], bird mating optimizer (BMO) [24], generalized oppositional teaching learning based optimization (GOTLBO) [29], artificial bee swarm optimization (ABSO) [28], genetic algorithm (GA) [18], and particle swarm optimization algorithm (PSO) [19].

**Table 2** Precise results for SDM of RTC France

Algorithm	$I_{ph}(A)$	$I_{sd1}(\mu A)$	$R_s(\Omega)$	$R_{sh}(\Omega)$	$n_1$	RMSE
SWOA	0.76077551	0.32302318	0.03637706	53.71886754	1.48110897	9.8602e-04
CWOA [8]	0.76077	0.3239	0.03636	53.7987	1.4812	9.8602e-04
WOA	0.76075413	0.32436114	0.03636524	54.10454052	1.481519944	9.8615e-04
PGJAYA [5]	0.7608	0.3230	0.0364	53.7185	1.4812	9.8602e-04
FPSO [4]	0.7607	0.3230	0.03637	53.7185	1.4811	9.8602e-04
IJAYA [6]	0.7608	0.3228	0.0364	53.7595	1.4811	9.8603e-04
BMO [4]	0.7607	0.3247	0.0363	53.8716	1.4817	9.8608e-04
GOTLBO [7]	0.7608	0.3297	0.0363	53.3664	1.4833	9.8856e-04
ABSO [3]	0.76080	0.30623	0.03659	52.2903	1.47583	9.9124e-04
PSO [1]	0.7607	0.400	0.0354	59.012	1.5033	1.38e-03
GA [2]	0.7619	0.8087	0.0299	42.3729	1.5751	1.8704e-02

Since no previous data are available for the accurate values of the parameters, the RMSE value is choosing as an index to demonstrate the precision of the parameter estimation. In this comparison, CWOA, FPSO, and PGJAYA methods were able to reach the lowest RMSE value like the SWOA method, and the GA method was able to reach the maximum value.

Tables 3 and 4 show the results for estimating seven parameters for the DDM and nine parameters for the TDM by SWOA and 10 other algorithms, respectively. As can be seen in Tables 3 and 4, the proposed algorithm was able to achieve a better RMSE than other algorithms. It can also be seen that the SWOA algorithm has achieved a lower RMSE value for the TDM than for the other two models. By looking closely at these results, two conclusions can be drawn: First, the TDM is a more accurate model for showing the performance of the RTC FRANCE cell, because in this model, most methods achieved a better RMSE than in the other two models, and second, the SWOA algorithm has a better ability to identify models with more unknown parameters, because it can get a better answer than other algorithms. However, as the number of unknown parameters increased, the rest of the algorithms performed worse, reaching very close RMSE values to the DDM. It should be noted that the best results for all algorithms in TDM were included in the table after 30 runs and were not taken from published results.

Since all meta-heuristic methods start with random points, for a fair comparison, it is necessary to run each method several times and then examine the results. Table 5 demonstrates the results of the studied algorithms during 30 runs. In the first part of this table, which is related to the SDM, it can be seen that most of the methods showed good stability and resistance. But when we increase the number of unknown parameters and move on to the TDM, the algorithms face a difficult challenge. This challenge has led to articles that offer new methods for identifying a cell or solar module parameters. As can be seen from Table 5, SWOA in all three models was able to show considerable stability compared to other algorithms. Also, note that the performance of the CWOA algorithm is also good compared to other algorithms.

Table 6 provides information on the estimated current by the SWOA algorithm and the relative error of all three models studied in this paper. To ensure the accuracy of the estimated parameters, it is sufficient to consider the relative error of the current obtained from Eq. (24). As you can see, given that the relative error value is very small, it can be concluded that the

**Table 3** Precise results for DDM of RTC France

Algorithm	$I_{ph}(A)$	$I_{sd1}(\mu A)$	$I_{sd2}(\mu A)$	$R_S(\Omega)$	$R_{sh}(\Omega)$	$n_1$	$n_2$	RMSE
SWOA	0.76078087	0.70757207	0.23082631	0.03671932	55.37109594	2	1.45271146	9.8249e-04
CWOA [8]	0.76077	0.24150	0.60000	0.03666	55.2016	1.45651	1.9899	9.8272e-04
WOA	0.76077727	0.26185068	0.22162798	0.03653061	54.34047408	1.46452503	1.82539530	9.8464e-04
PGJAYA [5]	0.7608	0.21031	0.88534	0.0368	55.8135	1.4450	2.0000	9.8263e-04
FPSO [4]	0.76078	0.22731	0.72786	0.036737	55.3923	1.45160	1.99969	9.8253e-04
LIAYA [6]	0.7601	0.00504	0.75094	0.0376	77.8519	1.2186	1.6247	9.8293e-04
BMO [4]	0.76078	0.21110	0.87688	0.03682	55.8081	1.44533	1.99997	9.8262e-04
GOTLBO [7]	0.7608	0.13894	0.26209	0.0365	53.4058	1.7254	1.4658	9.8742e-04
ABSO [3]	0.076078	0.26713	0.38191	0.03657	54.6219	1.46512	1.98152	9.8344e-04
PSO [1]	0.7623	0.4767	0.0102	0.0325	43.1034	1.5172	2	1.6600e-03
GA [2]	0.7608	0.0001	0.0001	0.0364	53.7185	1.3355	1.481	3.6040e-01

**Table 4** Precise results for TDM of RTC France

Algorithm	$I_{ph}(A)$	$I_{sd1}(\mu A)$	$I_{sd2}(\mu A)$	$I_{sd3}(\mu A)$	$R_s(\Omega)$	$R_{sh}(\Omega)$	$n_1$	$n_2$	$n_3$	RMSE
SWOA	0.76078285	0.24204643	0.36359195	1	0.03672224	55.69461854	1.45602655	2	2.40819703	9.8033e-04
CWOA	0.7607	0.2231	0.7390	0.2226	0.0367	55.6554	1.4497	2	2.5771	9.8204e-04
WOA	0.76077	0.2353	0.2213	0.4573	0.03668	55.4448	1.4543	1.4978	2	9.8249 e-04
PGJAYA	0.7607	0.2144	0.8059	0.1178	0.0368	55.7500	1.4464	2	2.2982	9.8234e-04
FPSO	0.7607	0.2225	0.7467	0.2353	0.0367	55.7531	1.4495	2	2.5851	9.8203e-04
LIAYA	0.7608	0.2349	0.2297	0.2297	0.0367	55.2641	1.4541	1.8695	2	9.8253 e-04
BMO	0.7607	0.2258	0.7504	7.9743e-08	0.0367	55.4885	1.4509	2	2.3144	9.8248e-04
GOTLBO	0.7607	0.2238	0.7583	0.0184	0.0367	55.4743	1.4501	2	2.3191	9.8245e-04
ABSO	0.7607	0.2001	0.5014	0.2102	0.0368	55.8344	1.4414	1.9156	2	9.8466e-04
PSO	0.7607	0.2259	0.7491	0.0023	0.0367	55.47571	1.4509	2	2.3156	9.8247e-04
GA	0.7605	0.3251	0.3608	0	0.0357	58.6086	1.4843	1.9975	2.2099	1.0531e-03

**Table 5** Comparison between RMSE values of SDM, DDM, TDM of RTC France obtained by different evolutionary methods after 30 runs

Algorithm	SWOA	CWOA	WOA	PGJAYA [5]	FPSO [24]	IJAYA [16]	BMO [53]	GOTLBO [29]	ABSO [28]	PSO [19]	GA [18]
SDM											
Min	9.8602e-04	9.8602e-04	9.8615e-04	9.8602e-04	9.8602e-04	9.8603e-04	9.8608e-04	9.8856e-04	9.9124e-04	1.38e-03	1.8704e-02
Mean	9.8602e-04	9.8605e-04	9.8641e-04	9.8602e-04	9.8604e-04	9.9204e-04	9.8651e-04	1.0450e-03	1.10102e-03	1.3915e-03	1.9416e-02
Max	9.8602e-04	9.8608e-04	9.8662e-04	9.8603e-04	9.8652e-04	1.0622e-03	9.8701e-04	1.2067e-03	1.2013e-03	1.4512e-03	2.0136e-02
DDM											
Min	9.8249e-04	9.8272e-04	9.8464e-04	9.8263e-04	9.8253e-04	9.8293e-04	9.8262e-04	9.8742e-04	9.8344e-04	1.6600e-03	3.6040e-01
Mean	9.8250e-04	9.8347e-04	9.8491e-04	9.8582e-04	9.8330e-04	1.0296e-03	9.9156e-04	1.1475e-03	9.8781e-04	2.0891e-03	4.1297e-01
Max	9.8251e-04	9.8406e-04	9.8514e-04	9.9499e-04	9.8401e-04	1.4055e-03	9.9546e-04	1.3947e-03	9.8802e-04	2.5106e-03	1.1325e-00
TDM											
Min	9.8033e-04	9.8204e-04	9.8249e-04	9.8234e-04	9.8203e-04	9.8293e-04	9.8248e-04	9.8245e-04	9.8466e-04	9.8247e-04	1.0531e-03
Mean	9.8051e-04	9.8301e-04	1.1141e-03	9.8641e-04	9.8589e-04	9.9512e-04	2.0047e-03	9.9469e-04	9.5160e-03	2.5841e-02	1.2508e-02
Max	9.8154e-04	9.8531e-04	1.2410e-03	9.9801e-04	9.8602e-04	1.1342e-03	5.4875e-03	3.4101e-03	1.6081e-02	4.9170e-02	1.5668e-02

**Table 6** Relative error for each measurement

DATA	$V_L(v)$	$I_L(A)$	SDM		DDM		TDM	
			$I_{e}(A)$	$R_{err}$	$I_{e}(A)$	$R_{err}$	$I_{e}(A)$	$R_{err}$
1	-0.2057	0.7640	0.76408760	-0.00011465	0.76399008	0.00001297	0.76397401	0.00003401
2	-0.1291	0.7620	0.76266261	-0.000086881	0.76260751	-0.000079662	0.76259936	-0.000078595
3	-0.0588	0.7605	0.76135471	-0.000112261	0.76133836	-0.000110117	0.76133730	-0.000109978
4	0.0057	0.7605	0.76015421	0.00045488	0.76017287	0.00043032	0.76017792	0.00042367
5	0.0646	0.7600	0.75905584	0.00124384	0.75910508	0.00117890	0.75911497	0.00116586
6	0.1185	0.7590	0.75804300	0.00126244	0.75811713	0.00116455	0.75813016	0.00114734
7	0.1678	0.7570	0.75709159	-0.00012098	0.75718241	-0.00024091	0.75719642	-0.00025941
8	0.2132	0.7570	0.75614208	0.00113459	0.75623775	0.00100794	0.75625016	0.00099151
9	0.2545	0.7555	0.75508733	0.00054650	0.75517180	0.00043460	0.75518002	0.00042370
10	0.2924	0.7540	0.75366448	0.00044517	0.75371884	0.00037302	0.75372085	0.00037036
11	0.3269	0.7505	0.75138807	-0.00118191	0.75139510	-0.00119125	0.75139020	-0.00118474
12	0.3585	0.7465	0.74734836	-0.00113516	0.74729885	-0.00106898	0.74728812	-0.00105464
13	0.3873	0.7385	0.74009689	-0.00215768	0.73999745	-0.00202359	0.73998379	-0.00200517
14	0.4137	0.7280	0.72739678	0.00082927	0.72727282	0.00099986	0.72726016	0.00101729
15	0.4373	0.7065	0.70695327	-0.00064116	0.70684321	-0.00048555	0.70683496	-0.00047389
16	0.4590	0.6755	0.67529488	0.00030374	0.67523460	0.00039304	0.67523249	0.00039617
17	0.4784	0.6320	0.63088429	0.00176848	0.63088813	0.00176237	0.63089129	0.00175736
18	0.4960	0.5730	0.57208205	0.00160457	0.57213739	0.00150769	0.57214328	0.00149737
19	0.5119	0.4990	0.49949163	-0.00098426	0.49956623	-0.00113345	0.49957193	-0.00114485
20	0.5265	0.4130	0.41349355	-0.00119362	0.41355265	-0.00133635	0.41355603	-0.00134451
21	0.5398	0.3165	0.31721950	-0.00226815	0.31724054	-0.00233434	0.31724086	-0.00233535
22	0.5521	0.2120	0.21210318	-0.00048647	0.21208244	-0.00038873	0.21208021	-0.00037820
23	0.5633	0.1035	0.10272136	0.00758008	0.10267418	0.00804308	0.10267081	0.00807618
24	0.5736	-0.0100	-0.00924884	0.08121640	-0.00929457	0.07589665	-0.00929730	0.07558095
25	0.5833	-0.1230	-0.12438135	-0.01110583	-0.12438980	-0.01117297	-0.12438999	-0.01117447
26	0.5900	-0.2100	-0.20919308	0.00385726	-0.20914935	0.00406716	-0.20914653	0.00408071



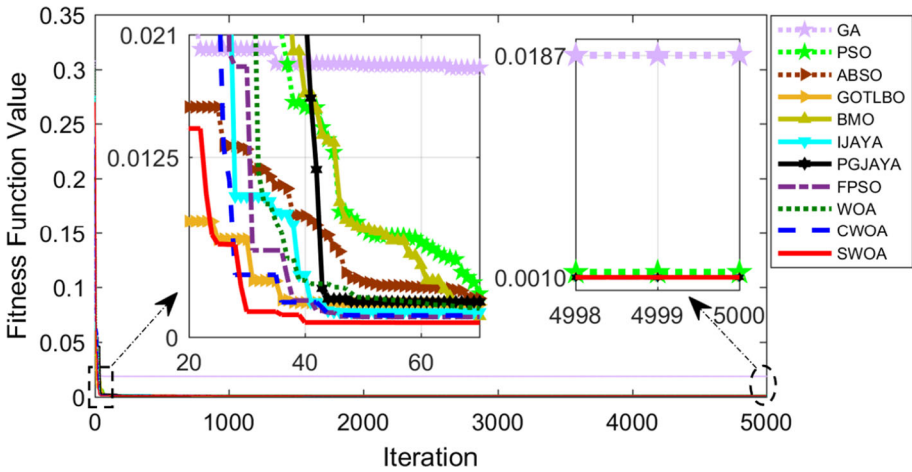


Fig. 7 RMSE evolution of the algorithms for the SD model of RTC France

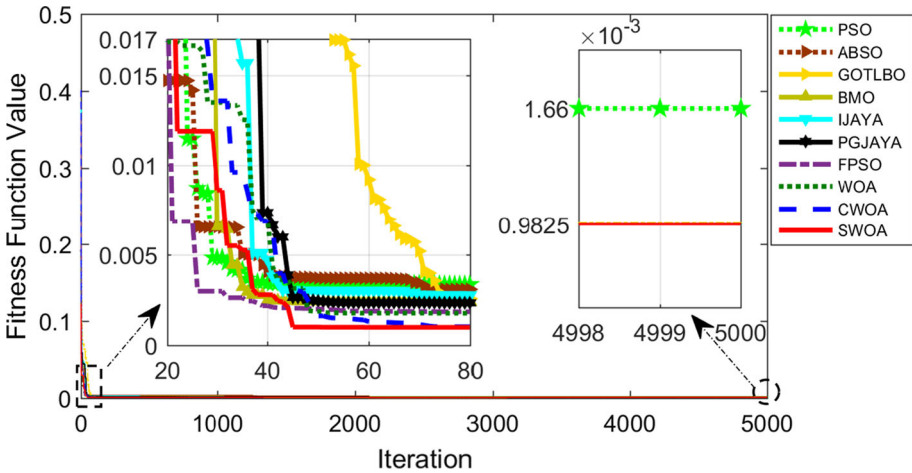
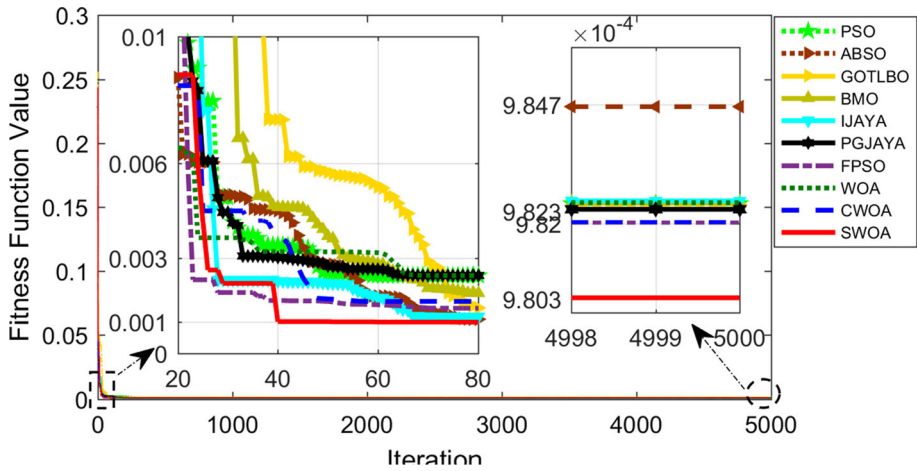


Fig. 8 RMSE evolution of the algorithms for the DD model of RTC France

parameters have been extracted correctly and the SWOA method was able to estimate the SDM, DDM, and TDM output current well.

$$R_{err} = \frac{I_L - I_{te}}{I_{te}} \tag{24}$$

Another factor that should be in a good way is the speed of getting the best answer. To show the convergence speed of the proposed algorithm, the cost function convergence process (RMSE) for SDM, DDM, and TDM is shown in Figs. 7, 8, and 9, respectively. To ensure that the SWOA has a high convergence rate, it was compared with all the algorithms in Table 5. As shown in Figs. 7, 8, and 9, the SWOA convergence rate is higher than other algorithms.



**Fig. 9** RMSE evolution of the algorithms for the TD model of RTC France

**Table 7** Detailed results for SDM of PWP201

Algorithm	$I_{ph}(A)$	$I_{sd1}(\mu A)$	$R_s(\Omega)$	$R_{sh}(\Omega)$	$n_1$	RMSE
SWOA	1.03051437	3.48221882	1.20127228	981.96750868	1.34999095	2.425074e-03
CWOA	1.03164979	3.09598060	1.21219669	827.54687808	1.33768079	2.451685e-03
WOA	1.03393368	2.49034859	1.23192419	644.59884712	1.31542184	2.635768e-03
JAYA	1.0307	3.4931	1.2014	1000	1.3514	2.42778e-03
STLBO	1.0305	3.4824	1.2013	982.0387	1.3511	2.42507e-03
TLABC	1.0305	3.4826	1.2013	982.1815	1.3512	2.42507e-03
CLPSO	1.0304	3.6131	1.1978	1000	1.3551	2.42806e-03
BLPSO	1.0305	3.5176	1.2002	992.7901	1.3522	2.42523e-03
DE/BBO	1.0303	3.6172	1.1969	1000	1.3552	2.42825e-03

### 5.2 Parameters identification of Photowatt-PWP201 PV module

In Table 7, the results for estimating 5 parameters for the SDM are given by SWOA and 9 other algorithms including WOA [30], CWOA [31], PGJAYA [26], JAYA [51], STLBO [8], TLABC [32], CLPSO [33], BLPSO [34], DE/BBO [52].

In this comparison, STLBO and TLABC methods were able to reach the lowest RMSE value like the SWOA method and WOA and CWOA methods reached the highest value. Note that these two methods performed relatively well in identifying the parameters of the RT. FRANCE system.

Tables 8 and 9 show the results for estimating seven parameters for the DDM and nine parameters for the TDM model by the SWOA and nine other algorithms, respectively. According to Table 8, the SWOA method obtained the lowest RMSE value compared to other methods.

Though the RMSE values acquired in the two WOA and SWOA algorithms in DDM are adjacent to each other, and even WOA achieves better results, when we challenge the algorithms and increase the number of parameters from 7 to 9 (TDM), we see that SWOA

**Table 8** Detailed results for DDM of PWP201

Algorithm	$I_{ph}(A)$	$I_{sd1}(\mu A)$	$I_{sd2}(\mu A)$	$R_s(\Omega)$	$R_{sh}(\Omega)$	$n_1$	$n_2$	RMSE
SWOA	1.031434	2.63811	1.0001e-06	1.235632	821.6525	1.320995	2.77788	2.0530e-03
CWOA	1.0332	2.6759	1.52820	1.23312	715.4537	1.5499	1.2844	2.2137e-03
WOA	1.0323	2.5129	1.0000e-06	1.2392	744.7153	1.3173	1.3173	2.0465e-03
JAYA	1.0326	2.6896	4.1973	1.2240	748.3831	1.3234	2.3680	2.2178e-03
STLBO	1.0328	2.5708	1.6899	1.2137	712.2977	1.3218	1.7314	2.2785e-03
TLABC	1.0331	2.6762	1.5280	1.2334	715.4478	1.5499	1.2832	2.2138e-03
CLPSO	1.0291	0.0010	9.3813	0.0314	75.6531	1.0000	1.5755	3.3925e-03
BLPSO	1.0265	9.2998	2.2586e-02	0.0301	1000	1.5225	1.4164	3.7559e-03
DE/BBO	1.0318	0.32774	2.4306e-06	1.2061	845.2495	1.3443	1.3443	2.400e-03

**Table 9** Detailed results for TDM of PWP201

Algorithm	$I_{ph}(A)$	$I_{sd1}(\mu A)$	$I_{sd2}(\mu A)$	$I_{sd3}(\mu A)$	$R_s(\Omega)$	$R_{sh}(\Omega)$	$n_1$	$n_2$	$n_3$	RMSE
SWOA	1.0305	3.4822e-06	1.0000e-6	1.0000e-6	1.2012	981.9781	1.4029	1.8671	2	2.0166e-03
CWOA	1.0305	3.4788	7.2209e-5	7.9930e-02	1.2005	992.7808	1.4032	1.9996	1.6487	2.4250e-03
WOA	1.0270	3.9028	2.0334e-4	6.0996e-02	1.1910	966.4183	1.4157	1.9992	1.6278	2.5814e-03
JAYA	1.0263	2.4380	8.4019	2.4413e-01	1.1911	710.7260	1.3885	1.8790	1.3544	2.7525e-03
STLBO	1.0327	0	5.3435	2.4748	1.1448	1000	1.8457	1.4547	1.9590	3.4186e-03
TLABC	1.0264	9.1106	2.0912e-02	6.3249e-02	1.0869	602.9147	1.5220	1.3011	1.5370	3.7258e-03
CLPSO	1.0419	3.43995	6.6266e-07	35.1499	1	755.0178	1.9938	1.2982	1.9987	9.9858e-03
BLPSO	1.0344	4.7853	1.16444	2.6812e-03	1	1000	2	1.5566	2	6.3626e-03
DE/BBO	1.0307	0	3.2036	3.1737	1.1952	996.3251	1.7749	1.3965	1.9564	2.4916e-03

algorithm showed excellent performance compared to other algorithms and WOA, along with other algorithms, has achieved even worse results than the DDM. However, the TDM is a more accurate model than the DDM. Examining Tables 7, 8, and 9, it is discernible that the SWOA algorithm has reached a lower RMSE value than the SDM and DDM. It should also be noted that the best results for all algorithms in the TDM were included in Table 9 after 30 runs and were not taken from another article.

Table 10 shows the results of the studied algorithms during 30 runs. In the first part of this table, which is related to the SDM, it can be seen that most of the methods showed good

**Table 10** Comparison between RMSE values of SDM, DDM, TDM of PWP201 obtained by different evolutionary methods after 30 runs

Algorithm	SWOA	CWOA	WOA	JAYA	STLBO	TLABC	CLPSO	BLPSO	DE/BBO
<b>SDM</b>									
Min	2.4250e-03	2.4516e-03	2.6357e-03	2.427e-03	2.4250e-03	2.4250e-03	2.4280e-03	2.4252e-03	2.4282e-03
Mean	2.4250e-03	2.4524e-03	2.7236e-03	2.5194e-03	2.5146e-03	2.4817e-03	2.6481e-03	2.4561e-03	2.4283e-03
Max	2.4250e-03	2.4556e-03	2.8201e-03	2.8171e-03	2.7419e-03	2.6134e-03	2.7194e-03	2.5104e-03	2.4284e-03
<b>DDM</b>									
Min	2.0530e-03	2.2137e-03	2.0465e-03	2.2178e-03	2.2785e-03	2.2138e-03	3.3925e-03	3.7559e-03	2.400e-03
Mean	2.0701e-03	2.3898e-03	2.8476e-03	3.2472e-03	2.7113e-03	2.3147e-03	3.4461e-03	4.2541e-03	3.4618e-03
Max	2.0950e-03	2.4250e-03	3.0151e-03	3.6218e-03	2.8669e-03	2.5634e-03	3.7684e-03	4.6119e-03	4.1284e-03
<b>TDM</b>									
Min	2.0166e-03	2.4250e-03	2.5814e-03	2.7525e-03	3.4186e-03	3.7258e-03	9.9858e-03	6.3626e-03	2.4916e-03
Mean	2.0301e-03	2.4431e-03	3.0105e-03	3.2225e-03	3.4315e-03	4.1060e-03	1.1320e-02	9.8649e-03	1.0514e-02
Max	2.1650-03	2.4619e-03	3.2315e-03	3.6642e-03	3.5994e-03	4.6119e-03	1.6131e-02	1.3112e-02	1.2549e-02

stability and resistance. It is very important to note that in practice, an algorithm is efficient that, in addition to quickly finding the optimal point, also has good stability. As you can see from Table 10, this algorithm did not show good stability, while SWOA showed very good stability.

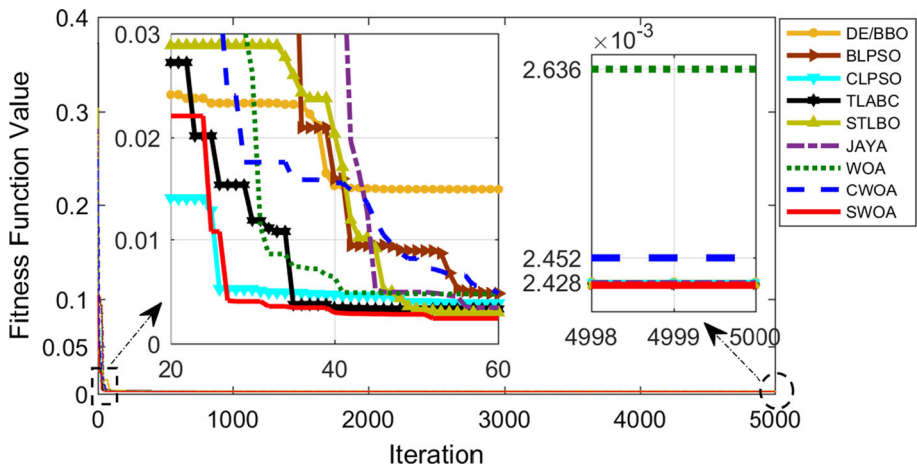
When we add to the number of unknown parameters and move on to the TDM, we are facing algorithms with a difficult challenge. But as can be seen from the table, SWOA in all three models was capable of demonstrating excellent stability compared to other algorithms and once again was able to succeed in this challenge. This success is due to SWOA's high ability to search globally. It should also be noted that the CWOA method showed good stability in the TDM but could not reach the minimum RMSE value, which shows the weakness of this algorithm in global search.

Table 11 is set up to ensure the accuracy of the parameters estimated by the SWOA. As you can see, the relative error value is very low, which points the exactitude of the identified parameters, and the SWOA method was able to estimate well the output current of the single-diode model, DDM, and TDM. Also, in this table, it can be seen that SWOA has reached a lower RMSE value with the TDM than the other two models. To prove it, it is sufficient to calculate the total value of the relative errors of each model separately and compare them with each other. It can be seen that the result of this sum in the model of TDM is less than the DDM and a SDM.

To show the convergence speed of the proposed algorithm, the cost function convergence process (RMSE) for single-diode, double-diode, and three-diode PWP201 models is shown in Figs. 10, 11, and 12, respectively. To ensure that the SWOA has a high convergence rate, it was compared with all the algorithms in Table 10. As can be seen from these figures, the SWOA convergence rate is higher than other algorithms.

**Table 11** Relative error for each measurement

DATA	$V_L(v)$	$I_L(A)$	SDM		DDM		TDM	
			$I_{re}(A)$	$R_{err}$	$I_{re}(A)$	$R_{err}$	$I_{re}(A)$	$R_{err}$
1	0.1248	1.0315	1.02912214	0.00231056	1.02913415	0.00229887	1.02986474	0.00158783
2	1.8093	1.0300	1.02738438	0.00254589	1.02745419	0.00247778	1.02778417	0.00215592
3	3.3511	1.0260	1.02574214	0.00025138	1.02573417	0.00025916	1.02584367	0.00015239
4	4.7622	1.0220	1.02410397	-0.00205445	1.02410103	-0.00205158	1.02312491	-0.00109948
5	6.0538	1.0180	1.02228338	-0.00419001	1.02014231	-0.00210001	1.02180506	-0.00372386
6	7.2364	1.0155	1.01991735	-0.00433109	1.01941831	-0.00384367	1.01951694	-0.00394004
7	8.3189	1.0140	1.01635076	-0.00231294	1.01724647	-0.00319142	1.01571486	-0.00168832
8	9.3097	1.0100	1.01049138	-0.00048628	1.01031843	-0.00031517	1.01004315	-0.00004272
9	10.2163	1.0035	1.00067872	0.00281936	1.00065473	0.00284340	1.00040487	0.00309387
10	11.0449	0.9880	0.98465332	0.00339883	0.98493476	0.00311212	0.98476472	0.00328533
11	11.8018	0.9630	0.95969740	0.00344128	0.95991837	0.00321030	0.96021830	0.00289694
12	12.4929	0.9255	0.92304877	0.00265557	0.92344862	0.00222143	0.92398779	0.00163661
13	13.1231	0.8725	0.87258819	-0.00010107	0.87247186	0.00003225	0.87342684	-0.00106115
14	13.6983	0.8075	0.80731016	0.00023514	0.80721973	0.00034720	0.80730449	0.00024217
15	14.2221	0.7265	0.72795785	-0.00200266	0.72715264	-0.00089752	0.72724318	-0.00102191
16	14.6995	0.6345	0.63646620	-0.00308925	0.63574691	-0.00196133	0.63569476	-0.00187945
17	15.1346	0.5345	0.53569608	-0.00223276	0.53516713	-0.00124658	0.53510716	-0.00113465
18	15.5311	0.4275	0.42881614	-0.00306925	0.42815627	-0.00153278	0.42800114	-0.00117088
19	15.8929	0.3185	0.31866864	-0.00052921	0.31825665	0.00076463	0.31809476	0.00127395
20	16.2229	0.2085	0.20785709	0.00309301	0.20795448	0.00262326	0.20817415	0.00156527
21	16.5241	0.1010	0.09835419	0.02690083	0.09795918	0.03104170	0.09799476	0.03066735
22	16.7987	-0.0080	-0.00816935	-0.02073040	-0.00846771	-0.05523453	-0.00863574	-0.07361731
23	17.0499	-0.1110	-0.11096846	0.00028415	-0.11142587	-0.00382200	-0.11101564	-0.00014088
24	17.2793	-0.2090	-0.20911761	-0.00056241	-0.20954826	-0.00261639	-0.20861489	0.00184603
25	17.4885	-0.3030	-0.30202235	0.00323699	-0.30259468	0.00133948	-0.30230147	0.00231070



**Fig. 10** RMSE evolution of the algorithms for the SD model of PWP201

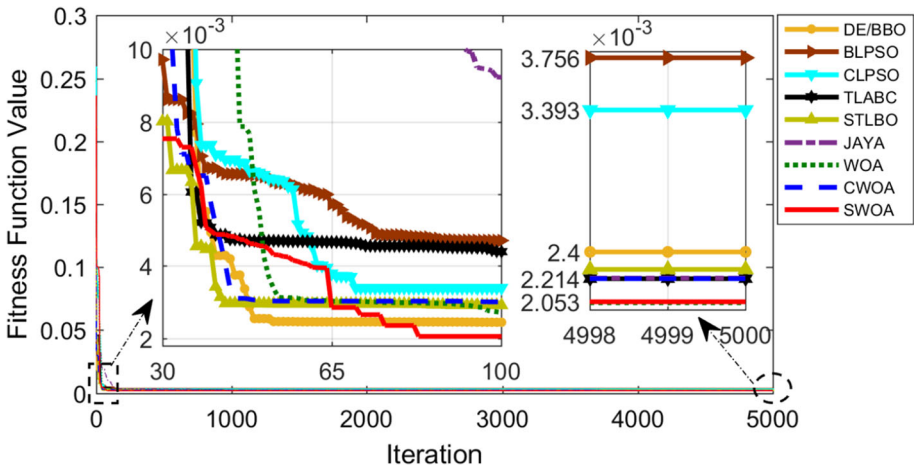


Fig. 11 RMSE evolution of the algorithms for the DD model of PWP201

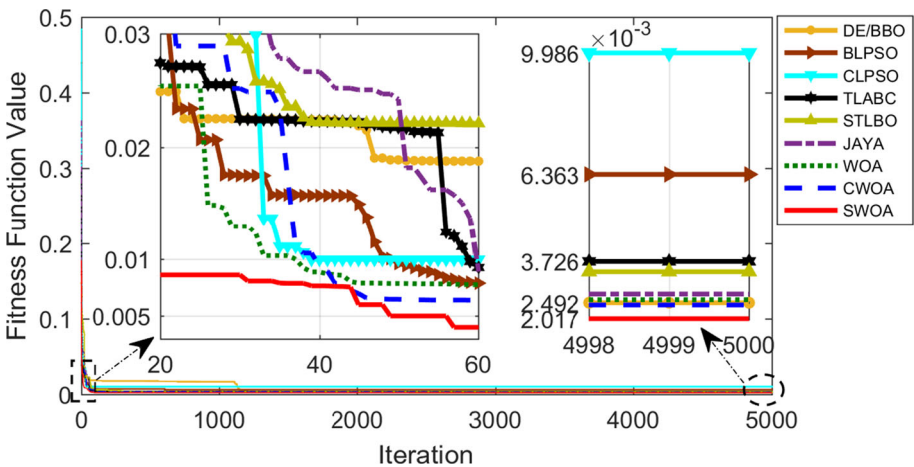


Fig. 12 RMSE evolution of the algorithms for the TD model of PWP201

### 5.3 Experimental test

In this section, the effect of temperature and radiation changes on voltage-current curves is investigated. In this regard, three different types of PV modules, called monocrystalline (SM55) module [54], multi-crystalline (KC200GT) module [55], and polycrystalline (SW255) module [49], have been taken into account. The experimental data of these solar modules, under STC, have been taken directly from the manufacturer’s datasheet, which is summarized in Table 12.

PV current is a function of temperature and radiation that can be written as Eq. (25):

$$I_{ph} = (I_{ph\_STC} + K_i \Delta T) \frac{G}{G_{STC}} \tag{25}$$

wherein  $I_{ph\_STC}$  is the light generated current at STC,  $\Delta T = T - T_{STC}$  ( $T_{STC} = 25^\circ\text{C}$ ),  $G$  is the surface irradiance of the cell, and  $G_{STC}$  ( $1000\text{w/m}^2$ ) is the irradiance at STC. The

**Table 12** STC specifications for the three modules used in the experiments

Parameters	SM55	KC200GT	SW255
Maximum power ( $P_{max}(W)$ )	55	200	255
Voltage at $P_{max}$ ( $V_{ppm}(V)$ )	17.4	26.3	31.4
Current at $P_{max}$ ( $I_{ppm}(A)$ )	3.15	7.61	8.15
Open-circuit voltage ( $V_{oc}(V)$ )	21.7	32.9	37.8
Short-circuit current ( $I_{sc}(A)$ )	3.45	8.21	8.66
$K_V$ (mV/°C)	- 76	-123	- 30
$K_i$ (mV/°C)	1.40	3.18	4
Number of cells	36	54	60

**Table 13** Identified parameters with the SWOA algorithm at STC

Parameters	SM55	KC200GT	SW255
$I_{ph}(A)$	3.46575503	8.21860582	8.67223408
$I_{sd1}(\mu A)$	2.26360312e-04	0.00143601	0.01620409
$R_s(\Omega)$	0.32241761	0.24093983	0.12261139
$R_{sh}(\Omega)$	311.82004454	774.212315	825.147321
$n_1$	1.0008282340	1.05528589	1.21928131
RMSE	0.02078510	0.01821364	0.01452717

constant  $K_i$  is the short-circuit current coefficient, normally provided by the manufacturer. The following equation can be used to describe the saturation flow with respect to temperature change [55].

$$I_{SD} = \frac{(I_{SC\_STC} + K_i \Delta T)}{\exp[q(V_{OC\_STC} + K_v \Delta T)/nkTN] - 1} \tag{26}$$

$K_v$  is coefficient of open-circuit voltage, the value of which is declared by the manufacturer.

From the values presented in the datasheet, the parameters of the selected PV modules are determined using the WHHO algorithm in MATLAB m\_script. The results obtained for the three investigated modules are given in Table 13. This table shows that the RMSE value of the proposed method is very small for all the three modules.

The current–voltage and power–voltage curves of the SM55 module are shown in Fig. 13 for different amounts of radiation at a constant temperature  $T = 25^\circ C$ . Figure 14 shows the specifications of the SM55 module for different temperature values at a constant radiation sun = 1000w/m<sup>2</sup>.

The I–V and P–V curves of the KC 200GT module are shown in Fig. 15 for various values of irradiance and at  $T = 25^\circ C$ . Figure 16 presents the I–V and the P–V characteristics of this module for different values of temperature and at an irradiance of sun = 1000w/m<sup>2</sup>.

Figure 17 describes I–V and P–V characteristics of the SW255 for ranging of irradiance from 200w/m<sup>2</sup> to 1000w/m<sup>2</sup> and at  $T = 25^\circ C$ . The I–V curve for different temperatures are not provided in the data sheet issued by the factory.

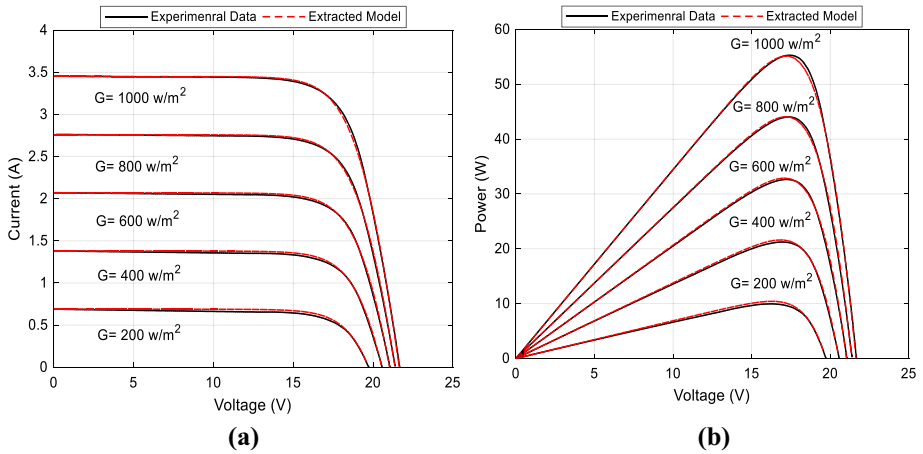


**Fig. 13** Comparison between the proposed method and the manufacturer Data of the SM55 module for different irradiances,  $T = 25\text{ }^\circ\text{C}$ , **a** I-V curve, **b** P-V curve

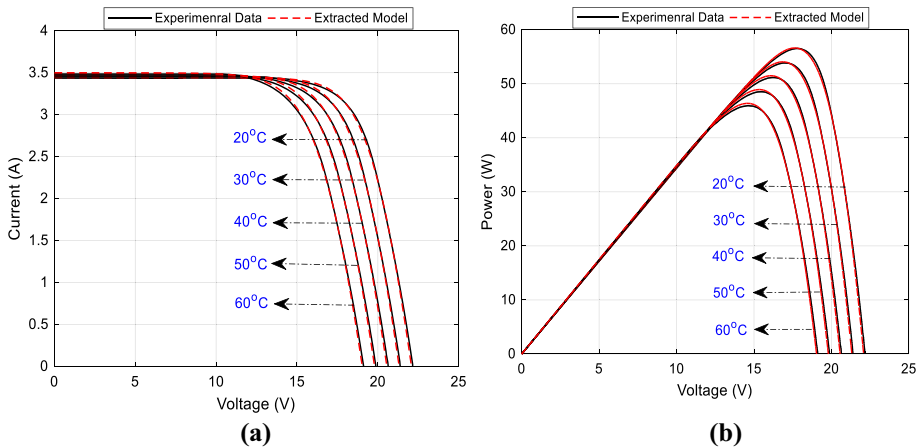


**Fig. 14** Comparison between the proposed method and the manufacturer Data of the SM55 module for different temperatures,  $G = 1000\text{ w/m}^2$ , **a** I-V curve, **b** P-V curve

### 5.4 The effects of the temperature and irradiance on the module parameters

In Table 14, the results for estimating the 5 parameters for the SDM are given by SWOA for the widely used SM55, KC200GT, and SW255 modules. Model inputs are radiation, temperature, series resistance, parallel resistance. The voltage-current (V-I) characteristic of photovoltaic cells depends on two factors: temperature and radiation. With decreasing temperature and increasing radiation, the output power increases, and with increasing temperature and decreasing radiation the output power decreases. Radiation and temperature are directly and inversely related to the output power, respectively. Tables 14 and 15 show that the estimated parameters  $I_{ph}(A)$  and  $I_{sd1}(\mu A)$  change with changing temperature or radiation conditions, but the variables  $R_s(\Omega)$ ,  $R_{sh}(\Omega)$  and  $n_1$  change under different conditions and remain almost constant. From a physical point of view, the parameter  $I_{ph}$  is photo-current and with increas-



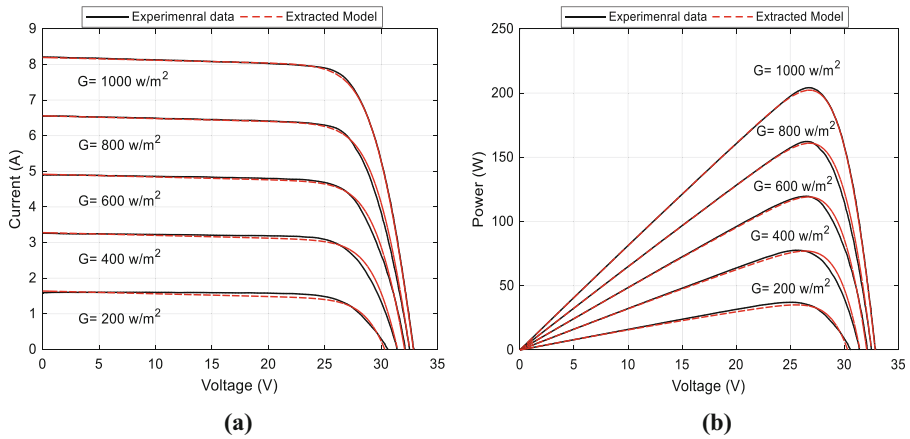


**Fig. 15** Comparison between the proposed method and the manufacturer Data of the KC 200GT module for different irradiances,  $T = 25\text{ }^\circ\text{C}$ , **a** I-V curve, **b** P-V curve

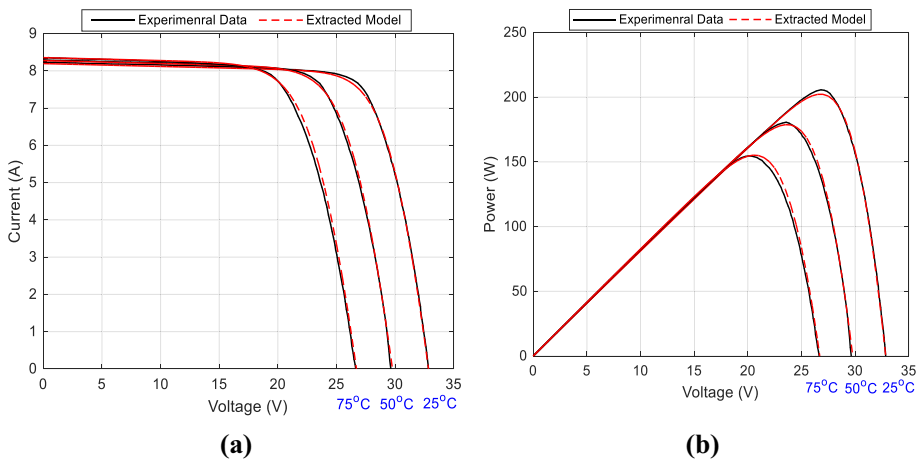


**Fig. 16** Comparison between the proposed method and the manufacturer Data of the KC 200GT module for different temperatures,  $G = 1000\text{ w/m}^2$ , **a** I-V curve, **b** P-V curve

ing radiation level, its value increases, which is observable in Table 14. The parameter  $I_{sd1}$  is the reverse saturation current of the diode and its value relies on the temperature. As the temperature gains, the quantity of photons absorbed increases and, as a result, their amount increases. This circumstance is certified by the results presented in Table 15 [26, 50].

Besides, it can be found that the resistance value of the  $R_s$  series for monocrystalline and multi-crystalline is less than 0.4.

With respect to the ideal factor of diode  $n_1$ , its value is almost fixed for a specific model under dissimilar circumstances, but its value is distinguished for different types of PV models [26]. It should be noted that the extracted results are close to the results of other methods [19, 24, 29].

**Table 14** Estimated optimal parameters by SWOA for three types of PV modules at different irradiance and temperature of 25 °C

Parameters	SM55	KC200GT	SW255
$G = 1000\text{w}/\text{m}^2$			
$I_{ph}(A)$	3.46575503	8.21860582	8.67223408
$I_{sd1}(\mu A)$	2.26360312e-04	0.00143601	0.01620409
$R_s(\Omega)$	0.32241761	0.24093983	0.12261139
$R_{sh}(\Omega)$	311.82004454	774.212315	825.147321
$n_1$	1.0008282340	1.05528589	1.21928131
RMSE	0.02078510	0.01821364	0.01452717
$G = 800\text{w}/\text{m}^2$			
$I_{ph}(A)$	2.77740892	6.57193101	6.93736802
$I_{sd1}(\mu A)$	4.49785556e-04	8.9120147e-04	0.01243336
$R_s(\Omega)$	0.33164013	0.32179412	0.14935662
$R_{sh}(\Omega)$	336.02512933	763.647913	846.784153
$n_1$	1.02415864	1.04264782	1.20698547
RMSE	0.01135360	0.02152142	0.01950175
$G = 1000\text{w}/\text{m}^2$			
$I_{ph}(A)$	2.07926408	4.82284077	5.208789881
$I_{sd1}(\mu A)$	2.71771063e-04	4.2146083e-03	0.009040316
$R_s(\Omega)$	0.33577536	0.31772024	0.201092676
$R_{sh}(\Omega)$	377.580024882	759.811947	923.1425146
$n_1$	1	1.08142513	1.191102785
RMSE	0.01120774	0.00710521	0.015320447
$G = 400\text{w}/\text{m}^2$			
$I_{ph}(A)$	1.38394610	3.31456952	3.476994332
$I_{sd1}(\mu A)$	3.24616001e-04	2.141771e-03	0.020786671
$R_s(\Omega)$	0.30977844	0.31223096	0.256109019
$R_{sh}(\Omega)$	334.02806096	761.347814	910.452136
$n_1$	1.00277773	1.06412677	1.245142018
RMSE	0.00783996	0.01022338	0.011781460
$G = 200\text{w}/\text{m}^2$			
$I_{ph}(A)$	0.68648791	1.67697515	1.746816956
$I_{sd1}(\mu A)$	0.02177540	4.4909963e-04	0.033177967
$R_s(\Omega)$	0.30933169	0.36141251	0.388661405
$R_{sh}(\Omega)$	369.56648088	720.314121	912.3147851
$n_1$	1.23756313	1.05124741	1.274607072
RMSE	0.00264573	0.00707896	0.009995405

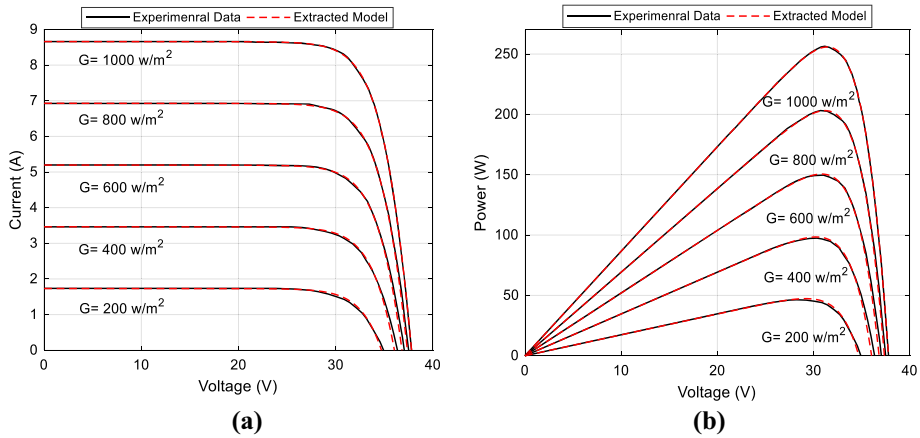


**Fig. 17** Comparison between the proposed method and the manufacturer Data of the SW255 module for different irradiances,  $T = 25\text{ }^\circ\text{C}$ , **a** I–V curve, **b** P–V curve

**Table 15** Optimal estimated parameters by WHHO for three modules at different temperature and constant irradiance of  $1000\text{ W/m}^2$

PV modules	Temperature	$I_{ph}(A)$	$I_{sd1}(\mu A)$	$R_s(\Omega)$	$R_{sh}(\Omega)$	$n_1$	RMSE
SM55	20 °C	3.43012610	0.15141237	0.32493172	458.1486	1.38416982	9.2631e-04
	30 °C	3.45167312	0.17954136	0.31647831	475.6415	1.37621438	9.0532e-04
	40 °C	3.46913647	1.06184731	0.31594137	511.3479	1.41213461	3.4263e-03
	50 °C	3.47816739	3.15948234	0.32153476	584.6174	1.38362494	3.4161e-03
	60 °C	3.49462817	6.84165721	0.32130415	498.2461	1.40346171	3.7561e-03
KC200GT	25 °C	8.21051643	2.23145e-03	0.34157893	765.3519	1.06158614	1.51238e-03
	50 °C	8.29314912	0.12638419	0.33614281	820.1674	1.08631425	2.6791e-03
	75 °C	8.37712648	1.64179431	0.33671429	806.9413	1.07641739	4.3149e-03

### 6 Conclusion

In this study, a novel improved optimization algorithm called springy whale optimization algorithm (SWOA) is proposed. SWOA has several advantages such as enhancing the performance, high convergence speed, global search capability, and high robustness over WOA. So as to look over the efficiency of SWOA, this algorithm is employed to estimate the parameters of SDM, DDM, TDM and also photovoltaic (PV) modules; the simulation results prove the supremacy of the presented algorithm. Moreover, the effectiveness of SWOA algorithm in the practical application has been assessed using commercial modules, including polycrystalline (SW255), multi-crystalline (KC200GT), and monocrystalline (SM55). This

evaluation is accomplished for different operating conditions under different irradiance and temperature conditions, which yield changes in the parameters of the PV model. Finally, the results obtained from various experimental tests confirming the high performance and robustness of the proposed algorithm.

## References

1. H.L. Tsai, Insolation-oriented model of photovoltaic module using Matlab/simulink. *Sol. Energy* **84**(7), 1318e26 (2010)
2. E. Saloux, A. Teyssedou, M. Sorin, Explicit model of photovoltaic panels to determine voltages and currents at the maximum powerpoint. *Sol. Energy* **85**(5), 713e22 (2011)
3. S. Ranjan et al., Silicon solar cell production. *Comput. Chem. Eng.* **35**(8), 1439–1453 (2011)
4. M.A. Green, Third generation photovoltaics: solar cells for 2020 and beyond. *Phys. E Low Dimen. Syst. Nanostruct.* **14**(1–2), 65–70 (2002)
5. X. Gao, Y. Cui, J. Hu, G. Xu, Z. Wang, J. Qu et al., Parameter extraction of solar cell models using improved shuffled complex evolution algorithm. *Energy Convers. Manag.* **157**, 460–479 (2018)
6. P.E. Campana, L. Wästhage, W. Nookuea, Y. Tan, J. Yan, Optimization and assessment of floating and floating-tracking PV systems integrated in on- and off-grid hybrid energy systems. *Sol. Energy* **177**, 782–795 (2019)
7. U.K. Das, K.S. Tey, M.Y.I. Idris, S. Mekhilef, M. Seyedmahmoudian, B. Horan et al., Forecasting of photovoltaic power generation and model optimization: a review. *Renew. Sustain. Energy Rev.* **81**, 912–928 (2018)
8. Q. Niu, H. Zhang, K. Li, An improved TLBO with elite strategy for parameters identification of PEM fuel cell and solar cell models. *Int. J. Hydrogen Energy* **39**, 3837–3854 (2014)
9. K. Ishaque, Z. Salam, H.S. Taheri, Modeling and simulation of photovoltaic (PV) system during partial shading based on a twodiode model. *Simul. Model Pract. Theory* **19**(7), 1613e26 (2011)
10. H. Patel, V. Agarwal, Matlab-based modeling to study the effects of partial shading on PV array characteristics. *IEEE Trans. Energy Convers.* **23**(1), 302e10 (2008)
11. Q. Niu, L. Zhang, K. Li, A biogeography-based optimization algorithm with mutation strategies for model parameter estimation of solar and fuel cells. *Energy Convers. Manag.* **86**, 1173–1185 (2014)
12. M. Abdelaziz, D. Oliva, Parameter estimation of solar cells diode models by an improved opposition-based whale optimization algorithm. *Energy Convers. Manag.* **171**, 1843–1859 (2018)
13. N. Pourmousa, S.M. Ebrahimi, M. Malekzadeh, M. Alizadeh, Parameter estimation of photovoltaic cells using improved Lozi map based chaotic optimization Algorithm. *Sol. Energy* **180**, 180–191 (2019)
14. N.E. Kohler, P.A. Turner PA, Shark tagging: a review of conventional methods and studies, in *The behavior and sensory biology of elasmobranch fishes: an anthology in memory of Donald Richard Nelson 2001* (pp. 191–224). Springer, Dordrecht.
15. E.A. Silver, R. Victor, V. Vidal, D. de Werra, A tutorial on heuristic methods. *Eur. J. Oper. Res.* **5**(3), 153–162 (1980)
16. K. Yu, J.J. Liang, B.Y. Qu, X. Chen, H. Wang, Parameters identification of photovoltaic models using an improved JAYA optimization algorithm. *Energy Convers. Manag.* **150**, 742–753 (2017)
17. I. Mukherjee, P.K. Ray, A review of optimization techniques in metal cutting processes. *ComputIndEng* **50**(1–2), 15–34 (2006)
18. M.R. AlRashidi, M.F. AlHajri, K.M. El-Naggar, A.K. Al-Othman, A new estimation approach for determining the I-V characteristics of solar cells. *Sol. Energy* **85**(7), 1543–1550 (2011)
19. M. Merchaoui, A. Sakly, M.F. Mimouni, Particle swarm optimisation with adaptive mutation strategy for photovoltaic solar cell/module parameter extraction. *Energy Convers. Manag.* **175**, 151–163 (2018)
20. S. Bana, R.P. Saini, Identification of unknown parameters of a single diode photovoltaic model using particle swarm optimization with binary constraints. *Renew. Energy* **101**, 1299–1310 (2017)
21. K. Et-Torabi, I. Nassar-Eddine, A. Obbadi, Y. Errami, R. Rmaily, S. Sahnoun, M. Agunaou, Parameters estimation of the single and double diode photovoltaic models using a Gauss-Seidel algorithm and analytical method: a comparative study. *Energy Convers. Manag.* **148**, 1041–1054 (2017)
22. V. Khanna, B.K. Das, D. Bisht, S.P.K. Vandana, A three diode model for industrial solar cells and estimation of solar cell parameters using PSO algorithm. *Renew. Energy* **78**, 105–113 (2015)
23. M.H. Qais, H.M. Hasanien, S. Alghuwainem, Identification of electrical parameters for three-diode photovoltaic model using analytical and sunflower optimization algorithm. *Appl. Energy* **250**, 109–117 (2019)

24. S.M. Ebrahimi, E. Salahshour, M. Malekzadeh, F. Gordillo, Parameters identification of PV solar cells and modules using flexible particle swarm optimization algorithm. *Energy* **179**, 358–372 (2019)
25. M.H. Qais, H.M. Hasanien, S. Alghuwainem, A.S. Noh, Coyote optimization algorithm for parameters extraction of three-diode photovoltaic models of photovoltaic modules. *Energy* **187**, 116001 (2019)
26. K. Yu, B. Qu, C. Yue, S. Ge, X. Chen, J. Liang, A performance-guided JAYA algorithm for parameters identification of photovoltaic cell and module. *Appl. Energy* **237**, 241–257 (2019)
27. S. Xu, Y. Wang, Parameter estimation of photovoltaic modules using a hybrid flower pollination algorithm. *Energy Convers. Manag.* **144**, 53–68 (2017)
28. A.A. Zadeh, A. Rezazadeh, Artificial bee swarm optimization algorithm for parameters identifications of solar cell modules. *Appl. Energy* **102**, 943–949 (2013)
29. X. Chen, K. Yu, W. Du, W. Zhao, G. Liu, Parameters identification of solar cell models using generalized oppositional teaching learning based optimization. *Energy* **99**, 170–180 (2016)
30. S. Mirjalili, A. Lewis, The whale optimization algorithm. *Adv. Eng. Softw.* **95**, 51–67 (2016)
31. D. Oliva, M. Abd El Aziz, A.E. Hassanien, Parameter estimation of photovoltaic cells using an improved chaotic whale optimization algorithm. *Appl. Energy* **200**, 141–154 (2017)
32. X. Chen, B. Xu, C. Mei, Y. Ding, K. Li, Teaching–learning–based artificial bee colony for solar photovoltaic parameter estimation. *Appl. Energy* **212**, 1578–1588 (2018)
33. J.J. Liang, A.K. Qin, P.N. Suganthan, S. Baskar, Comprehensive learning particle swarm optimizer for global optimization of multimodal functions. *IEEE Trans. Evolut. Comput.* **10**(3), 281–295 (2006)
34. X. Chen, H. Tianfield, C. Mei, W. Du, G. Liu, Biogeography-based learning particle swarm optimization. *Soft Comput.* **21**(24), 7519–7541 (2017)
35. B. Nayak, S. Sahu, Parameter estimation of DC motor through whale optimization algorithm. *Int. J. Power Elect. Drive Syst.* **10**(1), 83 (2019)
36. Mirjalili, S., Mirjalili, S.M., Saremi, S. and Mirjalili, S.: Whale optimization algorithm: theory, literature review, and application in designing photonic crystal filters, in *Nature-Inspired Optimizers* (pp. 219–238). Springer, Cham (2020).
37. D.T. Bui, S. Ghareh, H. Moayedi, H. Nguyen, Fine-tuning of neural computing using whale optimization algorithm for predicting compressive strength of concrete. *Eng. Comput.* pp.1–12 (2009)
38. I. Aljarah, H. Faris, S. Mirjalili, Optimizing connection weights in neural networks using the whale optimization algorithm. *Soft Comput.* **22**(1), 1–15 (2018)
39. M.H. Qais, H.M. Hasanien, S. Alghuwainem, Enhanced whale optimization algorithm for maximum power point tracking of variable-speed wind generators. *Appl. Soft Comput.* **86**, 105937 (2020)
40. S. Gupta, K. Saurabh, Modified artificial killer whale optimization algorithm for maximum power point tracking under partial shading condition, in *Proceedings of the 2017 International Conference on Recent Trends in Electrical, Electronics and Computing Technologies (ICRTEECT)* (pp. 87–92). IEEE. (2017)
41. Y. Chen, R. Vepa, M.H. Shaheed, Enhanced and speedy energy extraction from a scaled-up pressure retarded osmosis process with a whale optimization based maximum power point tracking. *Energy* **153**, 618–627 (2018)
42. Y. Cao, Y. Li, G. Zhang, K. Jermstittiparsert, M. Nasserri, An efficient terminal voltage control for PEMFC based on an improved version of whale optimization algorithm. *Energy Rep.* **6**, 530–542 (2020)
43. L. Liu, L. Wu, Predicting housing prices in China based on modified Holt’s exponential smoothing incorporating whale optimization algorithm. *Soc. Econ Plan. Sci.* **72**, 100916 (2020)
44. Z. Alameer, M. AbdElaziz, A.A. Ewees, H. Ye, Z. Jianhua, Forecasting gold price fluctuations using improved multilayer perceptron neural network and whale optimization algorithm. *Resour. Policy* **61**, 250–260 (2019)
45. N. Rana, M.S.A. Latiff, S.I.M. Abdulhamid, H. Chiroma, Whale optimization algorithm: a systematic review of contemporary applications, modifications and developments. *Neural Comput. Appl.* 1–33 (2020)
46. D.B. Prakash, C. Lakshminarayana, Optimal siting of capacitors in radial distribution network using whale optimization algorithm. *Alexand. Eng. J.* **56**(4), 499–509 (2017)
47. J. Nasiri, F.M. Khyabani, A whale optimization algorithm (WOA) approach for clustering. *Cogent Math. Stat.* **5**(1), 1483565 (2018)
48. X. Chen, K. Yu, W. Du, W. Zhao, G. Liu, Parameters identification of solar cell models using generalized oppositional teaching learning based optimization. *Energy* **99**, 170–180 (2016)
49. Y. Chaibi, M. Salhi, A. El-Jouni, A. Essadki, A new method to extract the equivalent circuit parameters of a photovoltaic panel. *Sol. Energy* **163**, 376–386 (2018)
50. A. Zekry, A. Shaker, M. Salem, Solar cells and arrays: principles, analysis, and design, in *Advances in Renewable Energies and Power Technologies* (pp. 3–56). Elsevier (2018).
51. R. Rao, Jaya: a simple and new optimization algorithm for solving constrained and unconstrained optimization problems. *Int. J. Ind. Eng. Comput.* **7**(1), 19–34 (2016)

52. W. Gong, Z. Cai, C.X. Ling, DE/BBO: a hybrid differential evolution with biogeography-based optimization for global numerical optimization. *Soft Comput.* **15**(4), 645–665 (2010)
53. A. Askarzadeh, A. Rezazadeh, Extraction of maximum power point in solar cells using bird mating optimizer-based parameters identification approach. *Sol. Energy* **90**, 123e33 (2013)
54. Shell SM55, Shell SM55 Solar PV Module Datasheet, 2002. [http://www.atlantasolar.com/pdf/Shell/ShellSM55\\_USv1.pdf](http://www.atlantasolar.com/pdf/Shell/ShellSM55_USv1.pdf).
55. Kyocera, KC200GT Kyocera PV module datasheet, 2019. [Online]. <http://www.kyocera.com.sg/products/solar/pdf/kc200gt.pdf>.